Technologies for Lightweight Structures 1(2) (2017), pp. 79–88
Special issue: 3rd International MERGE Technologies Conference (IMTC),
21st–22nd September 2017, Chemnitz

Technologies for
Lightweight Structures

High-performance machining of fiber-reinforced materials with hybrid ultrasonic-assisted cutting

Andrea Stoll[1], Carlo Rüger[2], Katja Busch[3], Thomas Mäder[4], Burkhard Kranz[5]

1) andrea.stoll@iwu.fraunhofer.de

2) carlo.rueger@iwu.fraunhofer.de

3) katja.busch@iwu.fraunhofer.de

4) thomas.maeder@iwu.fraunhofer.de

5) burkhard.kranz@iwu.fraunhofer.de

Fraunhofer IWU, Reichenhainer Straße 88, 09126 Chemnitz, Germany

Keywords

Cutting, Drilling, Fiber-reinforced, Hybrid, Milling, Ultrasonic-assisted

Abstract

A main approach for sustainable and efficient products is the application of innovative materials like fiber-reinforced plastics. Despite the excellent properties, the machining requirements, especially the hard cutting conditions, restrain the wide application of these materials. Thus a major task is the realization of the required part qualities combined with efficient machining strategies. The project ULTRASPAN, a joint venture of partners from industry and research institutes funded by the BMBF, attends to this challenge. The goal is the development of new hybrid machining concepts and process technologies for enhanced cutting of composite materials with ultrasonic-assistance. Prior condition is the development of novel robust actuators. Therefore, prototypic actuators for longitudinal and torsional vibration systems are developed in the project. Besides the novel actuator concepts, the results of ultrasonic-assisted drilling (UAD) on composite parts are presented in this paper. Machining tests in drilling of fiber-reinforced plastics with the novel prototype actuator systems were performed. Focus of the investigation was the influence of the ultrasonic vibration support on the bore quality. The superimposition of drilling with ultrasonic vibrations influences the process characteristics and engagement of the cutting edge. Machining tests showed the potential to enhance the bore quality with UAD in a certain parameter field.

1 Development of ultrasonic actuator

1.1 Preliminary considerations

A tool integrated ultrasonic actuator to be used for hybrid ultrasonic-assisted cutting has to superimpose harmonic high frequency vibrations (preferable above 20 kHz) on the main movements (cutting speed and feed) of the cutting tool. To achieve the highest possible ultrasonic amplitudes, resonant systems are commonly used. Usually, piezo ceramic transducers are applied for these applications. Because the ultrasonic actuator should be utilized to investigate not only the overall influence of ultrasonic assistance on the cutting process, but also in detail which kind of vibration is most suitable, two types of actuators are considered according to *Figure 1*: longitudinal (left) and torsional (right) actuator.

Digital Object Identifier: http://dx.doi.org/10.21935/tls.v1i2.83
www.lightweight-structures.de

The main points during the development of an ultrasonic actuator are finding and adjusting of eigenmodes of the system which

- correspond to the intended directional type,
- can be excited by the applied piezo ceramic transducers, and
- transform the electric excitation energy to mechanical kinetic energy of the tool efficiently.

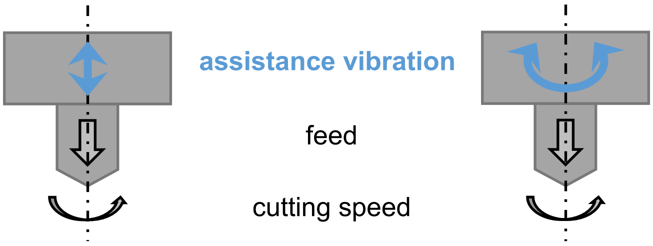

Figure 1: Considered directional types of ultrasonic assistance; Left: assistance vibration in feed direction – longitudinal actuator; Right:assistance vibration in speed direction – torsional actuator

That is why the development of the ultrasonic actuator was supported by finite element simulations (using the finite element system ANSYS® [1]) taking into account the piezo-mechanical behavior of the piezo ceramic transducers. With the finite element model, the eigenfrequencies and corresponding eigenforms of the ultrasonic unit were determined considering two different sets of electric boundary conditions:

- s.c. short circuit conditions, and
- o.c. open circuit conditions.

The effective electro-mechanical coupling coefficient (EEMC, k_{eff}), which is a measure of energy conversion between electric and mechanical energy [2], can be evaluated by:

$$k_{\text{eff}}^2 = \frac{f_{\text{o.c.}}^2 - f_{\text{s.c.}}^2}{f_{\text{o.c.}}^2} ,$$

where $f_{\text{o.c.}}$ is the eigenfrequency with open circuit conditions, and $f_{\text{s.c.}}$ is the eigenfrequency with short circuit conditions.

As piezo material SONOX® P8 [3] is applied, which is especially suitable for ultrasonic processing by low dielectric loss, high quality factor and maximum allowable stress.

Below, models and results are shown exemplarily for a drill bit with a diameter of 7 mm and a total length of 117 mm. For homogeneous cylindrical shafts with constant cross section, the natural frequencies of longitudinal and torsional vibrations are dependent on elastic material parameter (Young's modulus for longitudinal case and shear modulus for torsional case), mass density, and shaft length only (beside the boundary conditions and order of eigenfrequency). Therefore, the tool length has essential influence on the actual eigen/resonance frequencies which can be realized by the ultrasonic actuator. Different cross sections of tool, tool holder, booster, or clamp bolt have influence on the corresponding eigenforms, i.e. of the essence on the harmonic amplitude at the tool center point (TCP).

1.2 Longitudinal actuator

1.2.1 Model

To excite longitudinal eigenforms by the piezo ceramic transducers, a stack of hollow cylindrical piezo ceramic disks with polarization in thickness direction is used. The d_{33}-(longitudinal)-effect of piezoelectricity is relevant. The polarization of adjoining disks alternates (see *Figure 2*) so that alternating electrodes can be used.

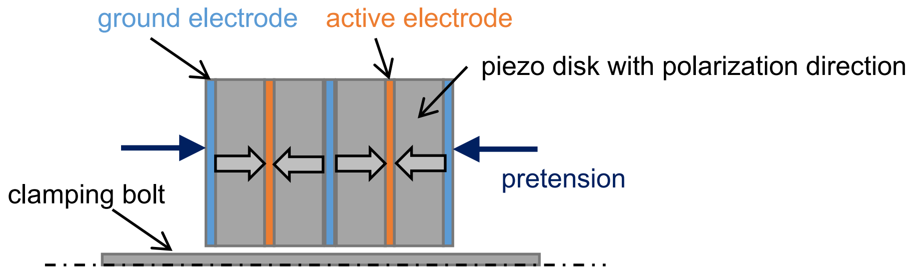

Figure 2: Polarization and electrodes for longitudinal actuator

Figure 3 shows the 3-D finite element model. Even though the main geometry and the intended eigenforms are axially symmetric (so a 2-D axially symmetric model would do), a 3-D model was generated to check whether non-symmetric eigenforms would interfere with the intended ones. Furthermore, the 3-D model can be used for the torsional actuator as well.

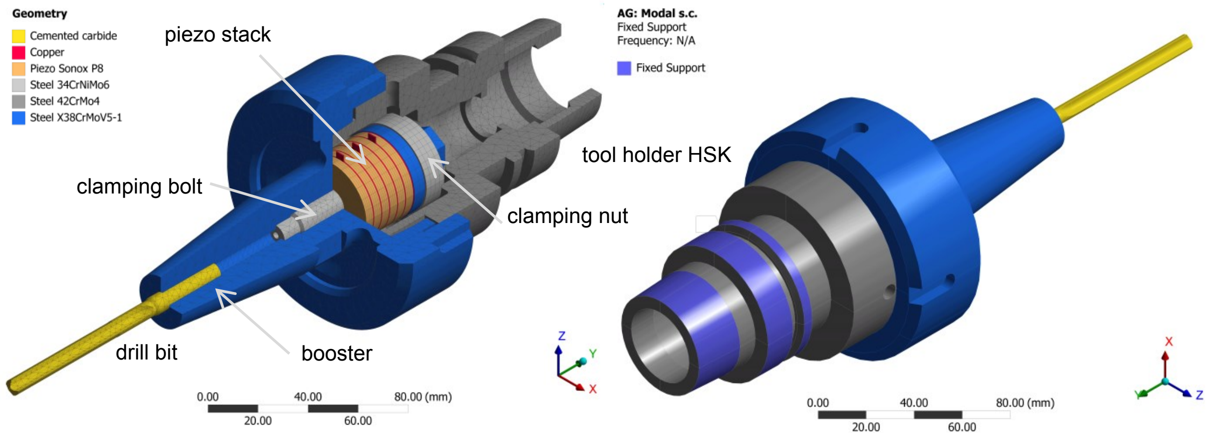

Figure 3: 3-D finite element model of longitudinal actuator and mechanical boundary condition

1.2.2 Modal results

Figure 4 contains views of the relevant eigenforms of the actuator (absolute value of total displacement normalized by mass matrix) which lead to longitudinal movement of the tool. The eigenforms for short circuit conditions are shown. The eigenforms for open circuit conditions differ only slightly.

The numbering respects only the relevant eigenmodes. In the considered frequency range from 10 to 35 kHz, an overall amount of 54 eigenmodes were found. The relevant longitudinal eigenmodes do not vary whether fixed (according Figure 3) or free mechanical boundary conditions are used. This is important to ensure that the connection of the actuator unit to the machine do not influence the ultrasonic vibration behavior.

In Figure 5, the eigenforms are shown as modal axial displacement along axial evaluation paths.

In Table 1, the eigenfrequencies, the corresponding EEMC, and the transformation ratios (γ, absolute ratio of axial displacements at TCP and clamping nut) are listed.

Table 1: List of eigenfrequencies, EEMC, and transformation ratios for longitudinal actuator

Mode	$f_{\text{s.c.}}$ / Hz	$f_{\text{o.c.}}$ / Hz	$EEMC$	γ
1	16119	16862	0.294	3.8
2	20263	21032	0.268	**9.1**
3	31291	34012	**0.392**	2.1

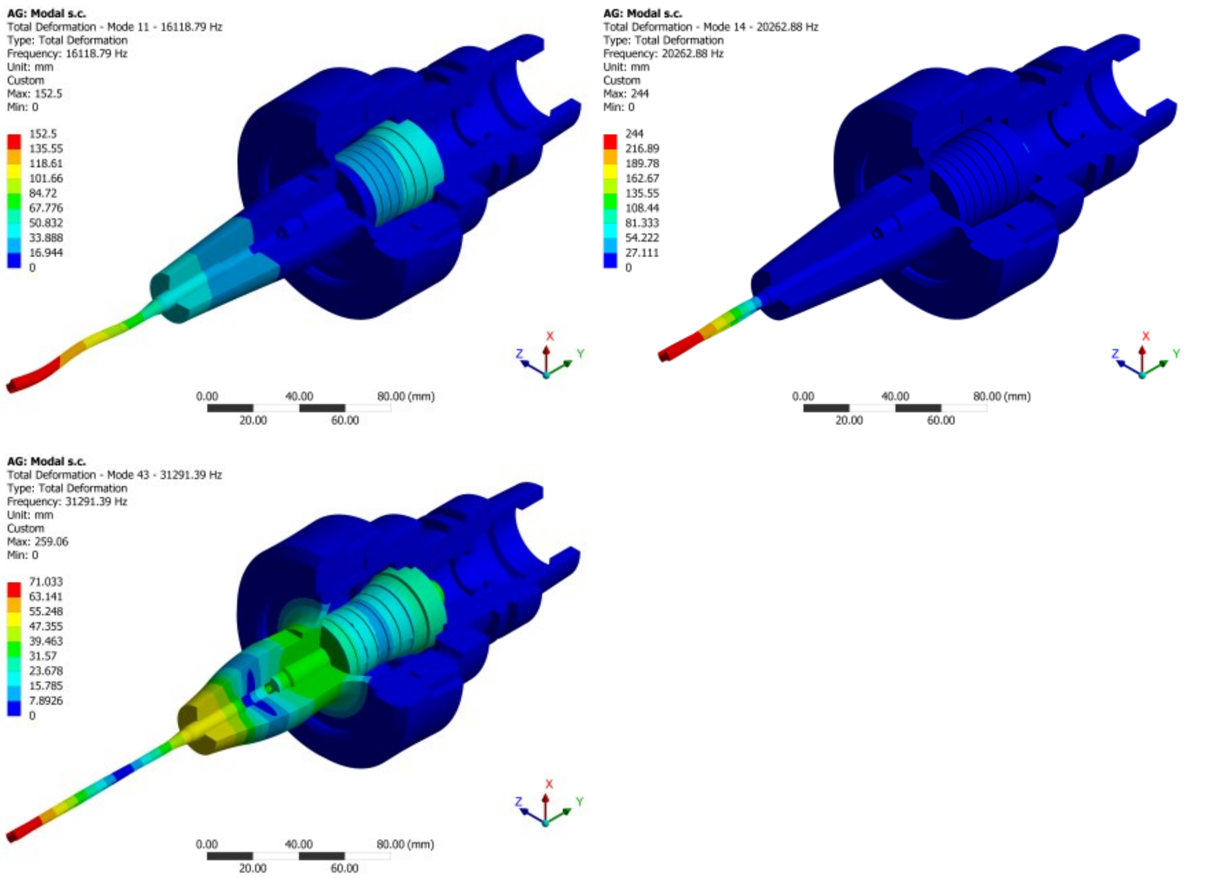

Figure 4: 1st to 3rd relevant eigenform of longitudinal actuator

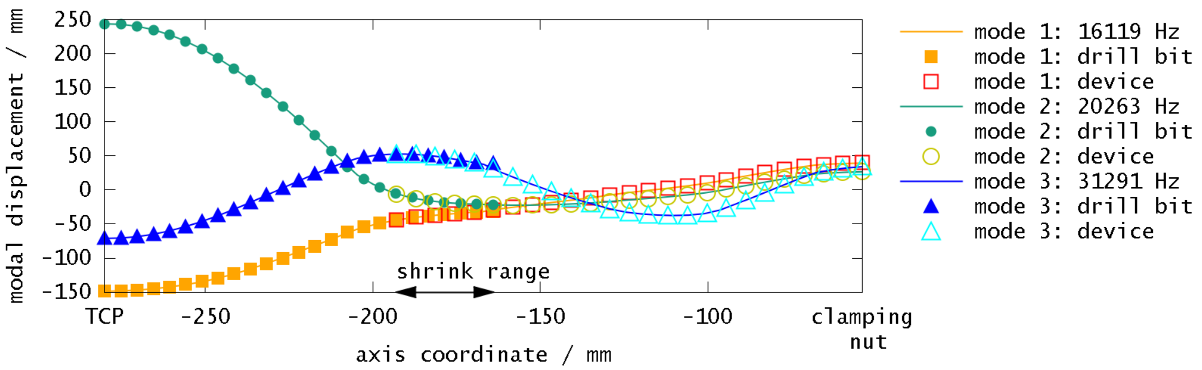

Figure 5: Modal axial displacement of 1st to 3rd relevant eigenform of longitudinal actuator

1.2.3 Harmonic results

To illustrate the effect of the eigenmodes on the dynamic operational behavior of the ultrasonic actuator, the frequency response of the axial displacement at the TCP and of the electric impedance was calculated (see Figure 6). Unity voltage amplitude (1 V) at the active electrode was used as excitation. A constant damping ratio of 0.01 was applied.

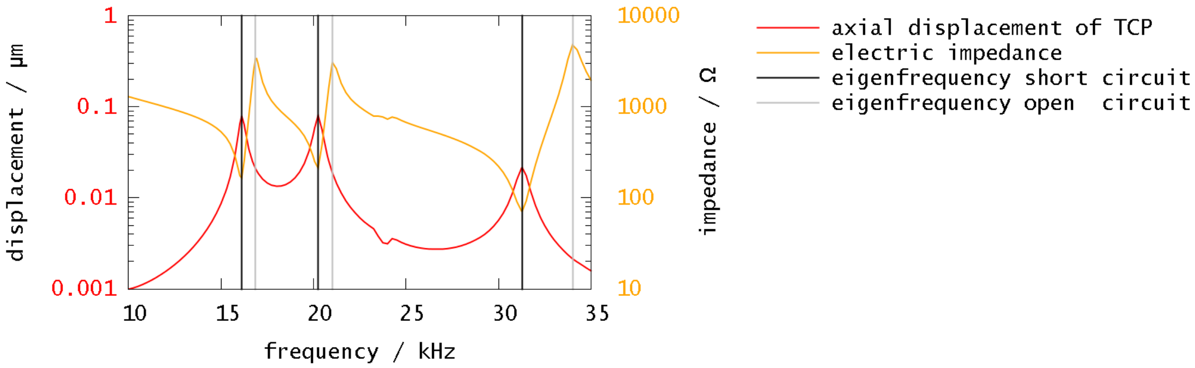

Figure 6: Magnitude frequency responses of longitudinal actuator due to unity voltage excitation

1.2.4 Evaluation of numerical results

The maxima of the TCP displacement amplitude are computed nearly at the short circuit eigenfrequencies. They correlate with the minima of the electric impedance. The maxima of the electric impedance amplitude conform to the open circuit eigenfrequencies.

For the 3rd relevant mode, the impedance minimum is lower and the impedance maximum is higher than the corresponding local extrema of the other two modes. This matches with the higher EEMC.

Despite this higher EEMC for the 3rd relevant mode, the TCP displacement resonance amplitude is lower because of the lowest transformation ratio. If the EEMC is a measure of overall energy conversion between electric and mechanical energy, the transformation ratio indicates whether the mechanical deformation affects the interesting TCP or other device parts.

Taking these considerations into account, mode 2 at around 21 kHz seems to be most suitable for excitation of ultrasonic assistance:

- The resonance frequency of mode 2 is higher than the common human frequency threshold of hearing (health protection).
- The transformation ratio of mode 2 is highest.
- The EEMC of mode 2 is not considerable lower than the EEMC of the other pairs.
- The modal displacement of mode 2 shows only low rate in cross direction (other than mode 1, see *Figure 1*).

1.3 Torsional actuator

1.3.1 Model

To excite torsional eigenforms of the device, torsional deformations of the piezo ceramic disks are necessary. Therefore, disks with polarization in tangential direction and operational electrodes at the facing surfaces should be used. This configuration exploits the d_{15}-(shear)-effect of piezoelectricity. A current development allows for poling of piezoelectric monolithic ring elements for torsional transducers [4]. The practical realization of this procedure is limited to thin piezo disks or ring elements. The finite element model of the torsional actuator uses the geometry of the longitudinal actuator (Figure 3) but thinner piezo disks and an ideal tangential polarization of the piezo disks. The alternation of the polarization direction of adjoining piezo disks is applied as described for the longitudinal actuator.

1.3.2 Modal results

The relevant modal results of the torsional actuator (eigenforms with high EEMC and eigenforms with high transformation ratio γ) are given in Figure 7, Figure 8, and

Table 2. In Figure 8 the eigenforms are shown as modal tangential displacement along axial evaluation paths with a radial distance of 3.5 mm from the rotating axis (radius of drill bit). Also, the transformation ratios γ in

Table 2 were evaluated based on the modal tangential displacements at TCP and clamping nut at the above given radial distance from the rotation axis.

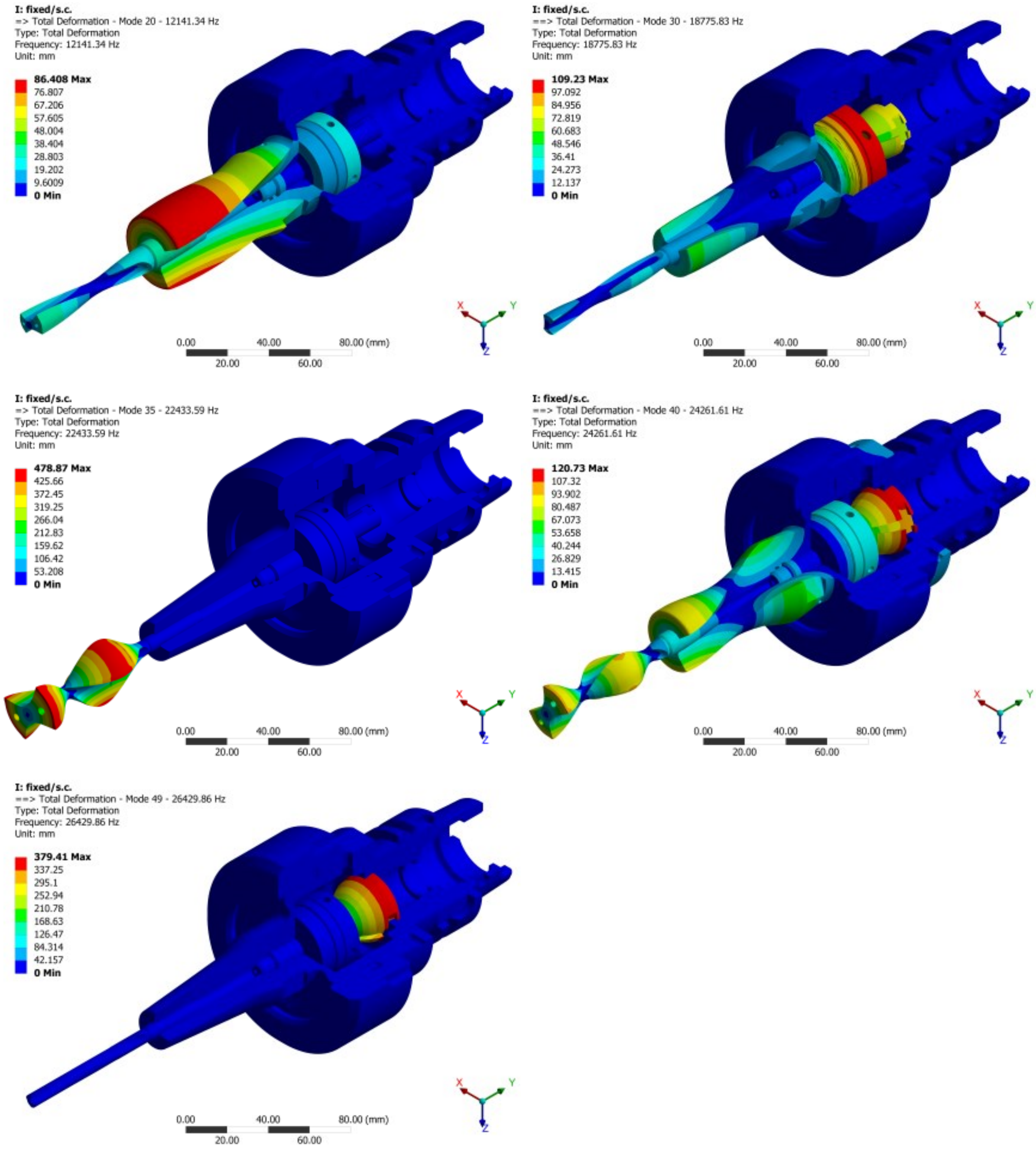

Figure 7: 1st to 5th relevant eigenform of torsional actuator

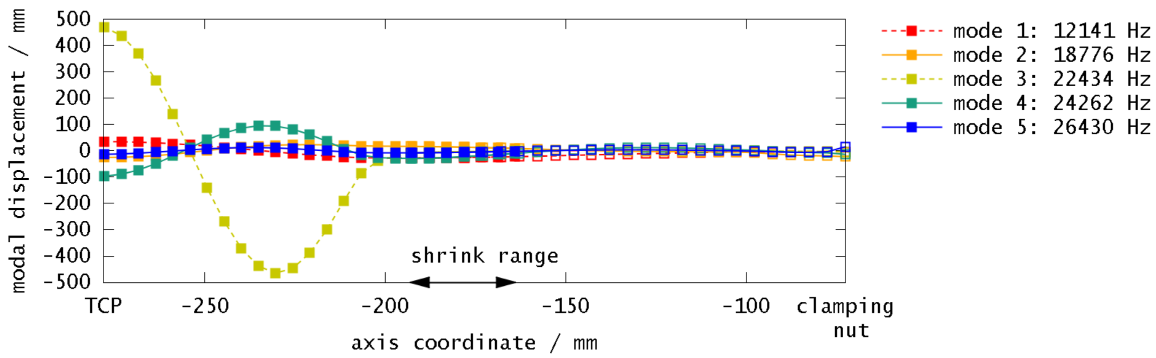

Figure 8: Modal tangential displacement of 1st to 5th relevant eigenform of torsional actuator

Table 2: List of eigenfrequencies, effective electro-mechanical coupling coefficients, and transformation ratios for torsional actuator

Mode pair	$f_{s.c.}$ / Hz	$f_{o.c.}$ / Hz	$EEMC$	γ
1	12141	12152	0.041	9.3
2	18776	19814	**0.319**	1.1
3	22434	22463	0.052	**146.2**
4	24262	24625	0.171	7.2
5	26430	26658	0.130	0.9

The 1st and 3rd mode show a low EEMC but a high transformation ratio. Mode 3 is in fact (the 2nd) torsional mode of the drill bit only, mode 1 is mainly a mode of the booster.

1.3.3 Harmonic results

All relevant eigenmodes shown in Figure 7 lead to displacement resonances in the harmonic analysis as can be seen in *Figure 9*. The magnitude of the respective resonance amplitude follows from a combination of EEMC and transformation ratio of the corresponding mode.

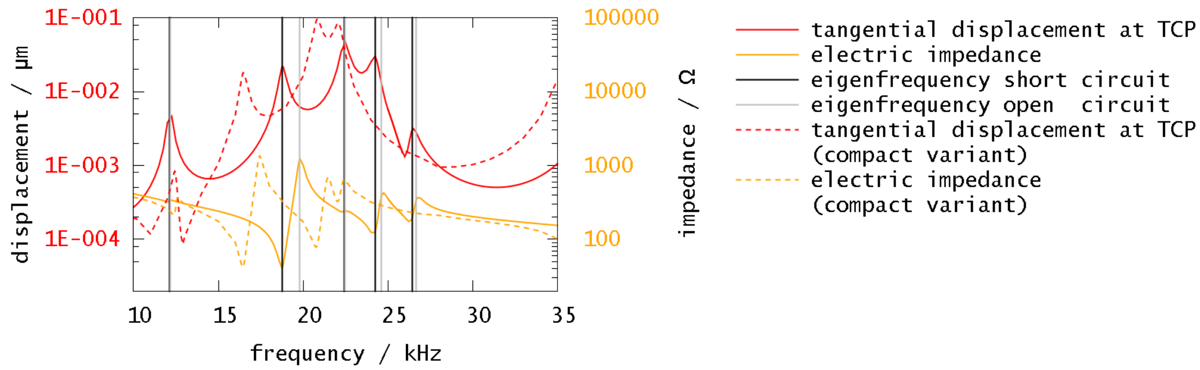

Figure 9: Magnitude frequency responses of torsional actuator due to unity voltage excitation

The modes with low EEMC (1st and 3rd mode) do not show clear influence on the impedance response, short circuit and open circuit eigenfrequency are nearly identical. The highest impedance jump is found for the 2nd mode as indicated by the highest EEMC.

In *Figure 9* the frequency responses of a more compact design variant of the torsional actuator are incorporated. A resonance shift to lower frequencies can be observed (disregarding mode 1, the 1st mode is only slightly influenced because this is mainly a drill bit mode only), but also higher resonance amplitudes. Also the influence on the impedance response is essential: The 3rd mode (in the original variant with nearly no effect to impedance) shows a considerable impedance jump in the compact variant.

1.3.4 Evaluation of numerical results

For the original variant, the 2nd and 4th mode are favorable for exciting torsional vibrations at the TCP. They both have comparable resonance amplitudes and influence on the impedance. The last point is of special interest because common ultrasonic generators providing the electric input signal are controlled by the impedance to find resonances. Even though the resonance amplitude of the 3rd mode is highest, it would not be possible to find it only by impedance measurement using frequency sweep without additional (mechanical) sensors.

2 Preparation and execution of machining experiments

2.1 Amplitude measurement

The longitudinal vibration system with the mounted tool showed resonance at 21.6 kHz. A single laser vibrometer Polytec CLV-2534 [5] was used for measuring the displacement on TCP which is the peak to peak vibration amplitude of the unloaded system. Figure 10 shows the experimental setup and the measurement results. With 75 % of the generator power level, a TCP displacement of 9.1 µm peak to peak was achieved. This was chosen as the operating point for the drilling tests. A further increase of the power level showed only marginal gain of amplitude but led to a notable heating of the actuator.

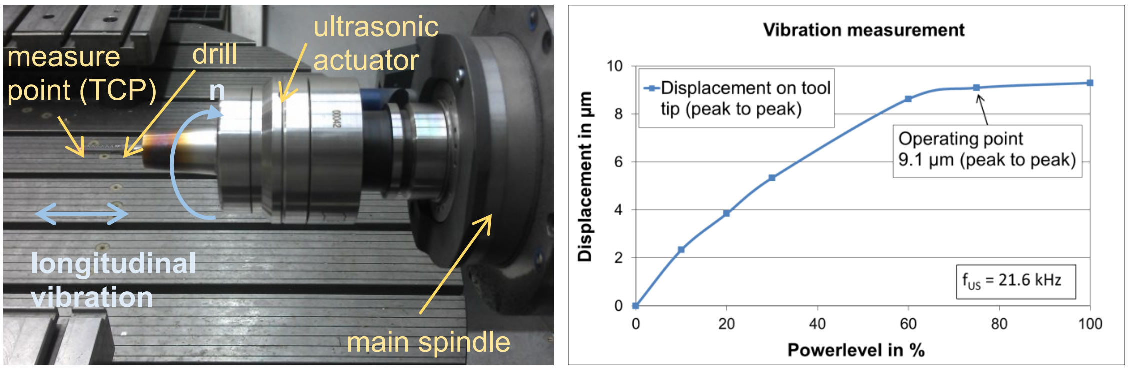

Figure 10: Measurement of displacement on the tool tip

2.2 Experimental setup

The drilling tools with the diameter of 5.05 mm and the point angle of 90° have two main cutting edges on the tool tip with straight slots and serrated guide chamfers. The tool material is solid tungsten carbide without coating. The tool shaft is mounted to the actuator by shrinking.

As test material a plastic matrix with plait of carbon and glass fibers is used. The workpieces are made of structure parts with a wall thickness of 3.5 mm. Brackets are used for clamping, and the bore exits are free and not covered by back-up support devices.

The cutting tests were done on a DMU 210 5-axis-machining center. The experiments were conducted under dry conditions without cooling. The operating point of the ultrasonic vibration system was set to 21.6 kHz with a generator power level of 75 %. The drilling tests were conducted with full factorial design, the parameter setup is shown in Table 3. 30 holes were drilled in each test row. To minimize the influence of tool wear for each test row, a new drill was used.

Table 3: Test parameters

v_c / m/min	f / mm	process influencing
190 (12.000 rpm)	0.02	no vibration (conventional / conv.)
317 (20.000 rpm)	0.04	ultrasonic assisted drilling (UAD)

2.3 Experimental results

For rating the results, the bore quality was evaluated with the help of a camera microscope. On both the entry and the exit side of the drilled holes, a certain area with errors, i.e. delamination or fiber pullout, is tolerated. The tolerance field for this investigation was set to ±1 mm radial from the circumference. Also protrusion of uncut fibers is feasible within this range. The quality of bore entries and exits was evaluated independently from each other. Figure 11 shows an overview of the bore quality according to the machining parameters. 30 holes were drilled with each parameter setup, so the maximum number within tolerance can be 30.

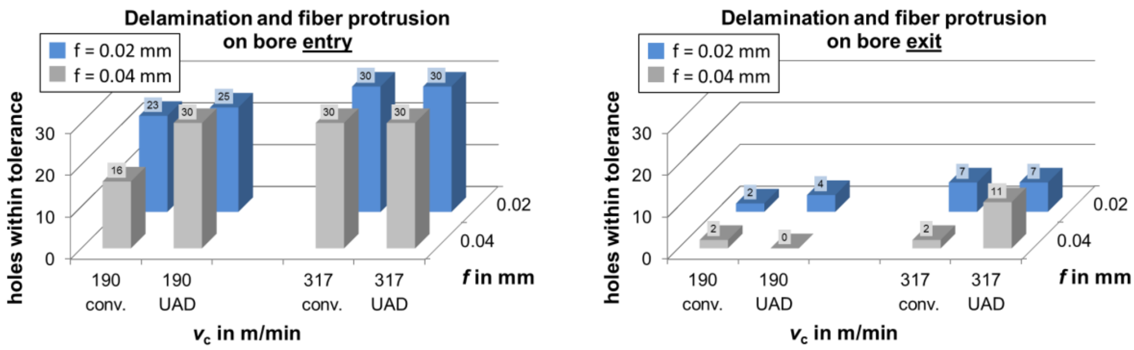

Figure 11: Entry and exit quality of manufactured holes

2.4 Evaluation of experimental results

The majority of the drilled holes show the bore entry side within tolerance. The main reason can be assumed in the feed direction which is pointed towards the material on the entry side. In particular the plait layers and also single fibers are supported by the underlying workpiece material and hence can be cut more safely. This appears advantageous for avoiding delamination and fiber pullout. Thus also fiber protrusion was found to be minimal on the entry side. UAD shows a significant increase of entry quality with the 190 m/min cutting speed. The lower feed rate of 0.02 mm tends to show better entry quality in conventional cutting, whereas the positive effects of UAD diminish. As an explanation approach, this could be due to an unfortunate relation between the values of amplitude and tool feed. This phenomenon has to be further investigated. The cutting speed of 317 m/min appears beneficial for the bore quality in general. All drilled holes are found within tolerance on entry side, so the influence of UAD cannot be rated here.

The quality of the bore exit side is much more critical than the entry side. The exits are characterized by delamination and fiber pullout as well as protrusion of uncut fibers or even fiber bundles. The main reason can be assumed in the missing back-up support of material. The fibers and even parts of the covering layers can bend away in front of the tool tip and avoid the cutting edges. The increase of cutting speed and application of a lower feed rate led only to small improvements of the exit quality. As seen on the bore entry side, the UAD shows no significant effects on feed 0.02 mm, whereas the combination of cutting speed 317 m/min, feed 0.04 mm and UAD made the best results in terms of the bore exit quality.

The experimental results show the potentials of UAD on fiber reinforced material. Approaches for further investigations are the optimization of feed and cutting speed with the longitudinal system and the application of torsional vibration system.

References

[1] SAS IP, Inc.: ANSYS Rev. 17.0 (2015).

[2] Trindade, M. A.; Benjeddou, Ay.: Effective Electromechanical Coupling Coefficients of Piezoelectric Adaptive Structures: Critical Evaluation and Optimization. Mech. of Adv. Mater. and Struct., 16(3) (2009), pp. 210–223. doi: 10.1080/15376490902746863

[3] CeramTec GmbH: Piezo-ceramic Transducers for Sonar and High-power Ultrasonic Applications. https://www.ceramtec.com/applications/piezo-applications/power-transducers/ (accessed 15 August 2017).

[4] Huang, M.: Model-based poling of piezoelectric monolithic ring elements for ultrasonic torsional transducers. Dissertation, Leibniz-Universität Hannover, 2013.

[5] Polytec GmbH: single point laser vibrometer. http://www.polytec.com/us/produkte/schwingungsmesssysteme/einpunkt-vibrometer/clv-2534-compact-laser-vibrometer/ (accessed 21 August 2017).